

Solving Out-Of-Equilibrium Quantum Problems via Time-Dependent Lanczos Method: I

Hantao Lu

Lanzhou University

CSRC Workshop on Quantum Non-Equilibrium Phenomena:
Methods and Applications, 17-21 June 2019



References (materials from)

- Hong-Yi Chen, *Exact Diagonalization: Introduction* (in a 2011 summer school).
- Anders W. Sandvik, *Exact Diagonalization Studies* (in a 2009 autumn school).
- Anders W. Sandvik, *Computational Studies of Quantum Spin Systems*, arXiv:1101.3281.



Outline

- 1 Introduction
- 2 Some Ingredients in ED
 - Basis Representation
 - Hamiltonian Matrix
 - Symmetries
 - Hamiltonian Matrix
 - Diagonalization Routines
- 3 Lanczos Algorithm
 - Basis of Lanczos
 - Loss of Orthogonality and Ghosts
- 4 Miscellaneous Applications
 - Green's Function
 - Finite Temperature Lanczos Methods
 - Time-Dependent Lanczos



Two Lattice Models

- Heisenberg $S = 1/2$ XXX chain

$$H = J \sum_{i=1}^N \mathbf{S}_i \cdot \mathbf{S}_{i+1} = J \sum_{i=1}^N \left[S_i^z S_{i+1}^z + \frac{1}{2} (S_i^+ S_{i+1}^- + S_i^- S_{i+1}^+) \right]$$

- Hubbard model

$$H = -t \sum_{\langle ij \rangle \sigma} c_{i\sigma}^\dagger c_{j\sigma} + U \sum_i n_{i\uparrow} n_{i\downarrow}$$



A 16×16 Matrix (Two-Site Hubbard Model)

$$H = \begin{pmatrix} 0 & 0 & 0 & 0 & 0 & 0 & 0 & 0 & 0 & 0 & 0 & 0 & 0 & 0 & 0 \\ 0 & 0 & 0 & 0 & -t & 0 & 0 & 0 & 0 & 0 & 0 & 0 & 0 & 0 & 0 \\ 0 & 0 & 0 & 0 & 0 & 0 & 0 & 0 & -t & 0 & 0 & 0 & 0 & 0 & 0 \\ 0 & 0 & 0 & U & 0 & 0 & -t & 0 & 0 & -t & 0 & 0 & 0 & 0 & 0 \\ 0 & -t & 0 & 0 & 0 & 0 & 0 & 0 & 0 & 0 & 0 & 0 & 0 & 0 & 0 \\ 0 & 0 & 0 & 0 & 0 & 0 & 0 & 0 & 0 & 0 & 0 & 0 & 0 & 0 & 0 \\ 0 & 0 & 0 & -t & 0 & 0 & 0 & 0 & 0 & 0 & 0 & -t & 0 & 0 & 0 \\ 0 & 0 & 0 & 0 & 0 & 0 & 0 & U & 0 & 0 & 0 & 0 & -t & 0 & 0 \\ 0 & 0 & -t & 0 & 0 & 0 & 0 & 0 & 0 & 0 & 0 & 0 & 0 & 0 & 0 \\ 0 & 0 & 0 & -t & 0 & 0 & 0 & 0 & 0 & 0 & 0 & -t & 0 & 0 & 0 \\ 0 & 0 & 0 & 0 & 0 & 0 & 0 & 0 & 0 & 0 & 0 & 0 & 0 & 0 & 0 \\ 0 & 0 & 0 & 0 & 0 & 0 & 0 & 0 & 0 & 0 & U & 0 & 0 & -t & 0 \\ 0 & 0 & 0 & 0 & 0 & 0 & -t & 0 & 0 & -t & 0 & U & 0 & 0 & 0 \\ 0 & 0 & 0 & 0 & 0 & 0 & 0 & -t & 0 & 0 & 0 & 0 & U & 0 & 0 \\ 0 & 0 & 0 & 0 & 0 & 0 & 0 & 0 & 0 & 0 & 0 & -t & 0 & 0 & U \\ 0 & 0 & 0 & 0 & 0 & 0 & 0 & 0 & 0 & 0 & 0 & 0 & 0 & 0 & 2U \end{pmatrix}$$



Why Use Exact Diagonalization?

Advantages:

- Robust, unbiased and completely versatile - almost anything can be calculated!
- There are models which are not easy to be accessed via other methods, e.g., frustrated magnets.
- Tiny error - numerical precision.
- Computational effort can be reduced by exploiting symmetries.
- Physical information about eigenstates.



Why Use Exact Diagonalization?

Advantages:

- Robust, unbiased and completely versatile - almost anything can be calculated!
- There are models which are not easy to be accessed via other methods, e.g., frustrated magnets.
- Tiny error - numerical precision.
- Computational effort can be reduced by exploiting symmetries.
- Physical information about eigenstates.

Especially useful if you want to get a maximum of physical information out of a finite system



Why Use Exact Diagonalization?

Advantages:

- Robust, unbiased and completely versatile - almost anything can be calculated!
- There are models which are not easy to be accessed via other methods, e.g., frustrated magnets.
- Tiny error - numerical precision.
- Computational effort can be reduced by exploiting symmetries.
- Physical information about eigenstates.

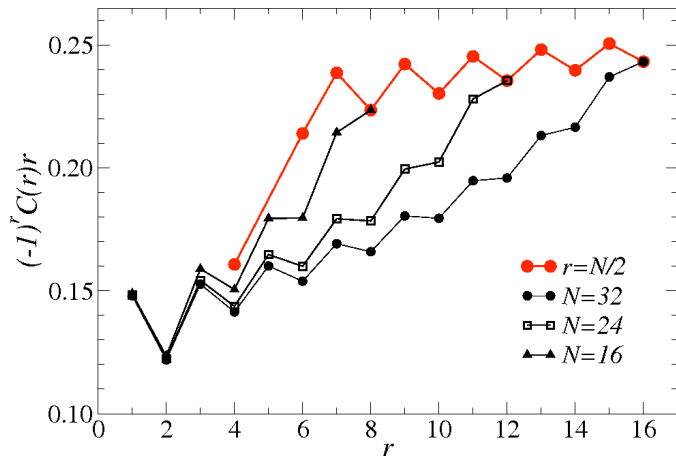
Especially useful if you want to get a maximum of physical information out of a finite system

Shortages:

- Expensive! The Hilbert space grows exponentially with the system size.
- Finite size effect. Sometimes hard to do scaling.



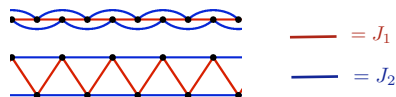
Illustration I: Heisenberg Chain



Spin correlations $C(r) = \langle \mathbf{S}_i \cdot \mathbf{S}_{i+r} \rangle$ for the Heisenberg chain. CFT prediction: $(-1)^r C(r) \propto \ln^{1/2}(r/r_0)/r$ for large r .



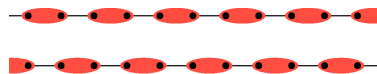
Illustration II: Heisenberg Chain with Frustrations



J_1 - J_2 model.

$$H = \sum_{i=1}^N [J_1 \mathbf{S}_i \cdot \mathbf{S}_{i+1} + J_2 \mathbf{S}_i \cdot \mathbf{S}_{i+2}]$$

$$g := J_2/J_1$$



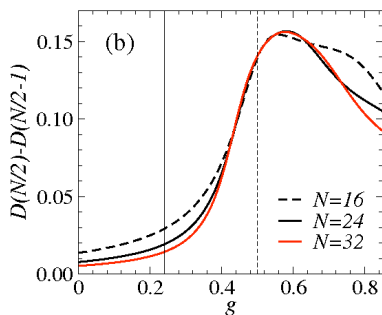
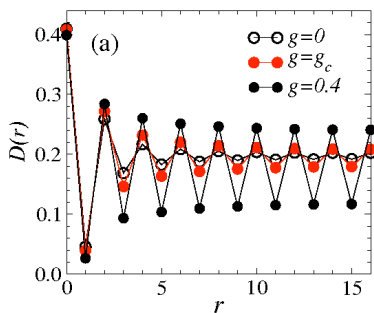
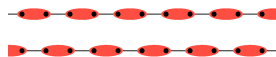
Valence-bond-solid (VBS) states.

- $g_c \approx 0.2411$: $g < g_c$, AFM, quasi-long range; $g > g_c$, VBS.
- Majumdar-Ghosh point: $g = 1/2$, with VBS as the exact (two-fold) ground state



Dimer correlations for VBS

$$D(r) = \langle B_i B_{i+r} \rangle = \langle (\mathbf{S}_i \cdot \mathbf{S}_{i+1}) (\mathbf{S}_{i+r} \cdot \mathbf{S}_{i+r+1}) \rangle$$

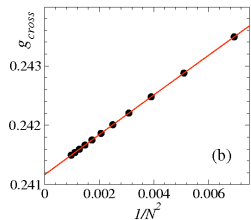
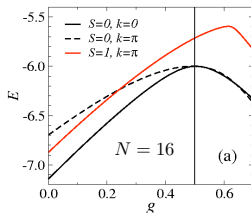


It is not easy to detect the transition in this way. Seems much larger systems are needed.



Determining the transition point using level crossings

- Lowest excitation for the Heisenberg chain ($g = 0$) is a triplet
 - ▶ this can be expected for all $g < g_c$
- The VBS state is two-fold degenerate for infinite N
 - ▶ and for any N at $g = 1/2$ (Majumdar-Ghosh point)
 - ▶ these two states are singlets
 - ▶ gap between them closes exponentially as $N \rightarrow \infty$
 - ▶ the lowest excitation is the second singlet



The two lowest excited states should cross at g_c .

Extrapolating point for different N up to 32 gives $g_c = 0.2411674(2)$.



Outline

- 1 Introduction
- 2 Some Ingredients in ED
 - Basis Representation
 - Hamiltonian Matrix
 - Symmetries
 - Hamiltonian Matrix
 - Diagonalization Routines
- 3 Lanczos Algorithm
 - Basis of Lanczos
 - Loss of Orthogonality and Ghosts
- 4 Miscellaneous Applications
 - Green's Function
 - Finite Temperature Lanczos Methods
 - Time-Dependent Lanczos



Outline

- 1 Introduction
- 2 Some Ingredients in ED
 - Basis Representation
 - Hamiltonian Matrix
 - Symmetries
 - Hamiltonian Matrix
 - Diagonalization Routines
- 3 Lanczos Algorithm
 - Basis of Lanczos
 - Loss of Orthogonality and Ghosts
- 4 Miscellaneous Applications
 - Green's Function
 - Finite Temperature Lanczos Methods
 - Time-Dependent Lanczos



Representation of Many-Body States

Mapping to (binary) integers:

- Spin-1/2 system
 - ▶ The basis of Hilbert space

$$|\uparrow\rangle \otimes \dots \otimes |\downarrow\rangle$$

- ▶ Three-site system (size $2^3 = 8$)

$ \downarrow\downarrow\downarrow\rangle = 000\rangle$	0
$ \downarrow\downarrow\uparrow\rangle = 001\rangle$	1
$ \downarrow\uparrow\downarrow\rangle = 010\rangle$	2
$ \downarrow\uparrow\uparrow\rangle = 011\rangle$	3
$ \uparrow\downarrow\downarrow\rangle = 100\rangle$	4
$ \uparrow\downarrow\uparrow\rangle = 101\rangle$	5
$ \uparrow\uparrow\downarrow\rangle = 110\rangle$	6
$ \uparrow\uparrow\uparrow\rangle = 111\rangle$	7

- Hubbard model
 - ▶ Four configuration for one site

$$|0\rangle \quad |\uparrow\rangle \quad |\downarrow\rangle \quad |\uparrow\downarrow\rangle$$

One site with two bits

- ▶ Two-site system (size $4^2 = 16$)
e.g., $N = 2$ and $S_z = 0$,

		$ 01\rangle_{\downarrow} 01\rangle_{\uparrow}$	5
		$ 01\rangle_{\downarrow} 10\rangle_{\uparrow}$	6
		$ 10\rangle_{\downarrow} 01\rangle_{\uparrow}$	9
		$ 10\rangle_{\downarrow} 10\rangle_{\uparrow}$	10
Site 1	Site 0	→ Binary	→ Decimal



Outline

- 1 Introduction
- 2 Some Ingredients in ED
 - Basis Representation
 - **Hamiltonian Matrix**
 - Symmetries
 - Hamiltonian Matrix
 - Diagonalization Routines
- 3 Lanczos Algorithm
 - Basis of Lanczos
 - Loss of Orthogonality and Ghosts
- 4 Miscellaneous Applications
 - Green's Function
 - Finite Temperature Lanczos Methods
 - Time-Dependent Lanczos



Outline

- 1 Introduction
- 2 Some Ingredients in ED
 - Basis Representation
 - Hamiltonian Matrix
 - **Symmetries**
 - Hamiltonian Matrix
 - Diagonalization Routines
- 3 Lanczos Algorithm
 - Basis of Lanczos
 - Loss of Orthogonality and Ghosts
- 4 Miscellaneous Applications
 - Green's Function
 - Finite Temperature Lanczos Methods
 - Time-Dependent Lanczos



Using Good Quantum Numbers

- Spin-1/2 system

$$H = J \sum_{i=1}^N \left[S_i^z S_{i+1}^z + \frac{1}{2} (S_i^+ S_{i+1}^- + S_i^- S_{i+1}^+) \right]$$

quantum number: $M_z = \sum_i S_i^z$

- Hubbard model

$$H = -t \sum_{\langle ij \rangle \sigma} c_{i\sigma}^\dagger c_{j\sigma} + U \sum_i n_{i\uparrow} n_{i\downarrow}$$

quantum numbers: N and S_z



Symmetries in ED

- Given a group G , $[H, G] = 0$
 - ▶ Basis can be regrouped according to different representations of G
 - ▶ Different representations can be labeled (e.g., by quantum numbers)
 - ▶ H is block diagonal (Hilbert space can be divided)



Symmetries in ED

- Given a group G , $[H, G] = 0$
 - ▶ Basis can be regrouped according to different representations of G
 - ▶ Different representations can be labeled (e.g., by quantum numbers)
 - ▶ H is block diagonal (Hilbert space can be divided)
- The inclusion of symmetries in an ED code has two major advantages:
 - ▶ Quantum number resolved energies and states
 - ▶ Reduction of the Hilbert space to be diagonalized



Symmetries in ED

- Given a group G , $[H, G] = 0$
 - ▶ Basis can be regrouped according to different representations of G
 - ▶ Different representations can be labeled (e.g., by quantum numbers)
 - ▶ H is block diagonal (Hilbert space can be divided)
- The inclusion of symmetries in an ED code has two major advantages:
 - ▶ Quantum number resolved energies and states
 - ▶ Reduction of the Hilbert space to be diagonalized
- Some examples:
 - ▶ U(1) related symmetries
 - ★ Conservation of particle numbers (N , U(1) gauge)
 - ★ Conservation of total S_z (M_z) (O(2) symmetry)
 - ▶ Spatial symmetry groups
 - ★ Point group (in general non-abelian)
 - ★ Translational symmetry (abelian, therefore 1D irreducible representations, branded with momentum k)



Example: Translational Symmetry

A state with momentum k can be constructed from any representative state $|a\rangle$ as (suppose the lattice size is N)

$$|a(k)\rangle = \frac{1}{\sqrt{N_a}} \sum_{r=0}^{N-1} e^{-ikr} \hat{T}^r |a\rangle$$

4-site examples
 $(0011) \rightarrow (0110) (1100) (1001)$
 $(0101) \rightarrow (1010)$

$$\left(\hat{T} |a(k)\rangle = \hat{T} \frac{1}{\sqrt{N_a}} \sum_{r=0}^{N-1} e^{-ikr} \hat{T}^r |a\rangle = e^{ik} |a(k)\rangle, \quad \text{i.e. momentum is } k \right)$$

Matrix elements

$$H |a(k)\rangle = \sum_{j=0}^N h_a^j e^{-iklj} \sqrt{\frac{N_{b_j}}{N_a}} |b_j(k)\rangle$$

The Hamiltonian matrix is block diagonal for different k . Each block size is reduced by $\sim 1/N$, compared with the original size D_{tot} .

For more details, see

Anders W. Sandvik, “Computational Studies of Quantum Spin Systems”, arXiv:1101.3281.



Outline

- 1 Introduction
- 2 Some Ingredients in ED
 - Basis Representation
 - Hamiltonian Matrix
 - Symmetries
 - **Hamiltonian Matrix**
 - Diagonalization Routines
- 3 Lanczos Algorithm
 - Basis of Lanczos
 - Loss of Orthogonality and Ghosts
- 4 Miscellaneous Applications
 - Green's Function
 - Finite Temperature Lanczos Methods
 - Time-Dependent Lanczos



Hamiltonian Matrix

- Matrix recalculation on the fly (matrix-free)

Hubbard model

- Sparse matrix

e.g., short-range interaction

- Dense matrix

ED in momentum space formulation & Quantum Hall problems



Sparse Matrix Storage

- Storage medium: RAM, hard disk
- Format:
 - 2D array: $H[i][j]$
 - Sparse matrix

For example (in column-style)

$$H = \begin{pmatrix} 0 & 0 & 0 & 0 & 0 & 0 & 0 & 0 & 0 & 0 & 0 & 0 & 0 & 0 & 0 & 0 \\ 0 & 0 & 0 & 0 & -t & 0 & 0 & 0 & 0 & 0 & 0 & 0 & 0 & 0 & 0 & 0 \\ 0 & 0 & 0 & 0 & 0 & 0 & 0 & 0 & -t & 0 & 0 & 0 & 0 & 0 & 0 & 0 \\ 0 & 0 & 0 & U & 0 & 0 & -t & 0 & 0 & -t & 0 & 0 & 0 & 0 & 0 & 0 \\ 0 & -t & 0 & 0 & 0 & 0 & 0 & 0 & 0 & 0 & 0 & 0 & 0 & 0 & 0 & 0 \\ 0 & 0 & 0 & 0 & 0 & 0 & 0 & 0 & 0 & 0 & 0 & 0 & 0 & 0 & 0 & 0 \\ 0 & 0 & 0 & -t & 0 & 0 & 0 & 0 & 0 & 0 & 0 & -t & 0 & 0 & 0 & 0 \\ 0 & 0 & 0 & 0 & 0 & 0 & 0 & U & 0 & 0 & 0 & 0 & -t & 0 & 0 & 0 \\ 0 & 0 & -t & 0 & 0 & 0 & 0 & 0 & 0 & 0 & 0 & 0 & 0 & 0 & 0 & 0 \\ 0 & 0 & 0 & -t & 0 & 0 & 0 & 0 & 0 & 0 & 0 & -t & 0 & 0 & 0 & 0 \\ 0 & 0 & 0 & 0 & 0 & 0 & 0 & 0 & 0 & 0 & 0 & 0 & 0 & 0 & 0 & 0 \\ 0 & 0 & 0 & 0 & 0 & 0 & 0 & 0 & 0 & 0 & 0 & U & 0 & 0 & -t & 0 \\ 0 & 0 & 0 & 0 & 0 & 0 & -t & 0 & 0 & -t & 0 & 0 & U & 0 & 0 & 0 \\ 0 & 0 & 0 & 0 & 0 & 0 & 0 & -t & 0 & 0 & 0 & 0 & 0 & U & 0 & 0 \\ 0 & 0 & 0 & 0 & 0 & 0 & 0 & 0 & 0 & 0 & 0 & -t & 0 & 0 & U & 0 \\ 0 & 0 & 0 & 0 & 0 & 0 & 0 & 0 & 0 & 0 & 0 & 0 & 0 & 0 & 0 & 2U \end{pmatrix}$$

Only nonzero elements are stored. We need three arrays:

- H , for nonzero elements
 $H[0] = -t$, $H[1] = -t$, $H[2] = U, \dots$
- BlockNo, the initiate position in H for each column
 $\text{BlockNo}[0] = 0$, $\text{BlockNo}[1] = 0$, $\text{BlockNo}[2] = 1$, $\text{BlockNo}[3] = 2, \dots$
- Bra-state Nf, for final states
 $\text{Nf}[0] = 4$, $\text{Nf}[1] = 8$, $\text{Nf}[2] = 3, \dots$



Outline

- 1 Introduction
- 2 **Some Ingredients in ED**
 - Basis Representation
 - Hamiltonian Matrix
 - Symmetries
 - Hamiltonian Matrix
 - **Diagonalization Routines**
- 3 Lanczos Algorithm
 - Basis of Lanczos
 - Loss of Orthogonality and Ghosts
- 4 Miscellaneous Applications
 - Green's Function
 - Finite Temperature Lanczos Methods
 - Time-Dependent Lanczos



Routines

- If H is dense or system small enough (thousand or several ten thousands),
 - ▶ Use
 - ★ Jacobi
 - ★ Householder
 - ★ LAPACK
 - ★ ...
 - ▶ All these apply orthogonal transformations to H until tridiagonal form, then quickly diagonalized.
 - ▶ Full diagonalization



Routines

- If H is dense or system small enough (thousand or several ten thousands),
 - ▶ Use
 - ★ Jacobi
 - ★ Householder
 - ★ LAPACK
 - ★ ...
 - ▶ All these apply orthogonal transformations to H until tridiagonal form, then quickly diagonalized.
 - ▶ Full diagonalization
- If H is sparse, huge, and only a few low-lying states are required,
 - ▶ Use
 - ★ ARPACK
 - ★ IETL/ALPS
 - ★ DiagHam
 - ★ ...
 - ▶ These are iterative solvers based on variants of Lanczos algorithm.



Outline

- 1 Introduction
- 2 Some Ingredients in ED
 - Basis Representation
 - Hamiltonian Matrix
 - Symmetries
 - Hamiltonian Matrix
 - Diagonalization Routines
- 3 Lanczos Algorithm
 - Basis of Lanczos
 - Loss of Orthogonality and Ghosts
- 4 Miscellaneous Applications
 - Green's Function
 - Finite Temperature Lanczos Methods
 - Time-Dependent Lanczos



Outline

- 1 Introduction
- 2 Some Ingredients in ED
 - Basis Representation
 - Hamiltonian Matrix
 - Symmetries
 - Hamiltonian Matrix
 - Diagonalization Routines
- 3 **Lanczos Algorithm**
 - **Basis of Lanczos**
 - Loss of Orthogonality and Ghosts
- 4 Miscellaneous Applications
 - Green's Function
 - Finite Temperature Lanczos Methods
 - Time-Dependent Lanczos



Basis of Lanczos

Krylov space

$$\mathcal{K} = \text{span}\{|\phi_0\rangle, H|\phi_0\rangle, \dots, H^M|\phi_0\rangle, \dots\}$$

Key message: In the iterative Krylov space, the H matrix is in a tridiagonal form.

$$H = \begin{pmatrix} a_0 & b_1 & 0 & \dots \\ b_1 & a_1 & b_2 & \dots \\ 0 & b_2 & a_2 & \dots \\ \vdots & \vdots & \vdots & \ddots \end{pmatrix}$$

C. Lanczos, J. Res. Natl. Bur. Stand. **45**, 255 (1950).



Simple Illustration

Start from a state $|\phi_0\rangle$. Suppose $\langle\phi_0|\phi_0\rangle = 1$ already, then $a_0 = \langle\phi_0|H|\phi_0\rangle$. Construct

$$|\phi'_1\rangle = H|\phi_0\rangle - |\phi_0\rangle\langle\phi_0|H|\phi_0\rangle = H|\phi_0\rangle - a_0|\phi_0\rangle, \quad (1)$$

where $|\phi'_1\rangle$ can be regarded as, geometrically, the component of $H|\phi_0\rangle$ perpendicular to $|\phi_0\rangle$. Then it's easy to see that

$$\langle\phi'_1|\phi'_1\rangle = \langle\phi_0|H|\phi'_1\rangle := b_1^2. \quad (2)$$

For *normalized* $|\phi_1\rangle$, $b_1 = \langle\phi_0|H|\phi_1\rangle$, and $a_1 = \langle\phi_1|H|\phi_1\rangle$.

Go ahead, we have

$$|\phi'_2\rangle = H|\phi_1\rangle - |\phi_1\rangle\langle\phi_1|H|\phi_1\rangle - |\phi_0\rangle\langle\phi_0|H|\phi_1\rangle = H|\phi_1\rangle - a_1|\phi_1\rangle - b_1|\phi_0\rangle. \quad (3)$$

The orthogonality of $|\phi'_2\rangle$ with $|\phi_1\rangle, |\phi_0\rangle$ has already been guaranteed. And similarly to Eq. (2),

$$\langle\phi'_2|\phi'_2\rangle = \langle\phi_1|H|\phi'_2\rangle := b_2^2, \quad (4)$$

so $b_2 = \langle\phi_1|H|\phi_2\rangle$, $a_2 = \langle\phi_2|H|\phi_2\rangle$. Importantly, note that

$$\langle\phi_0|H|\phi_2\rangle = (\langle\phi'_1| - a_0\langle\phi_0|)\phi_2 = 0. \quad (5)$$

For $|\phi'_3\rangle$,

$$|\phi'_3\rangle = H|\phi_2\rangle - |\phi_2\rangle\langle\phi_2|H|\phi_2\rangle - |\phi_1\rangle\langle\phi_1|H|\phi_2\rangle = H|\phi_2\rangle - a_2|\phi_2\rangle - b_2|\phi_1\rangle. \quad (6)$$

Due to Eq. (5), $\langle\phi_0|\phi'_3\rangle = 0$. Accordingly, one can be easily convinced that the Hamiltonian matrix in the Krylov space generated by the above procedure is indeed a tridiagonal matrix.



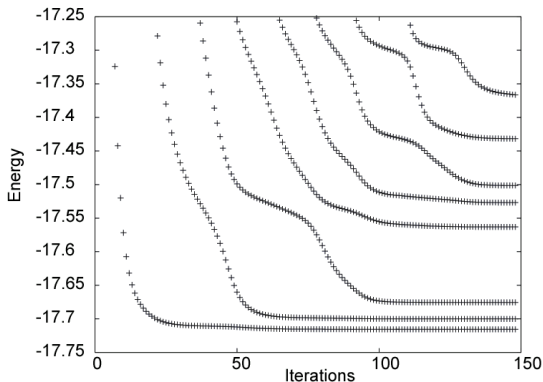
The Convergence of Lanczos

- Eigenvalues of H_N converge rapidly towards eigenvalues of H .
- Once desired eigenvalue is converged, restart recursion and assemble the eigenvector.



The Convergence of Lanczos

- Eigenvalues of H_N converge rapidly towards eigenvalues of H .
- Once desired eigenvalue is converged, restart recursion and assemble the eigenvector.



Ground state converges first, then successively excited states.



Some Words

- Degeneracies of eigenvalues can not be resolved by construction.
- The Lanczos method can only generate a **single** state of a multiplet.
some random linear combination of degenerate states
- To resolve the degeneracies a band Lanczos or the (Jacobi-)Davidson technique is needed.
- The orthogonality will be eventually lost with the increase of iteration ...



Outline

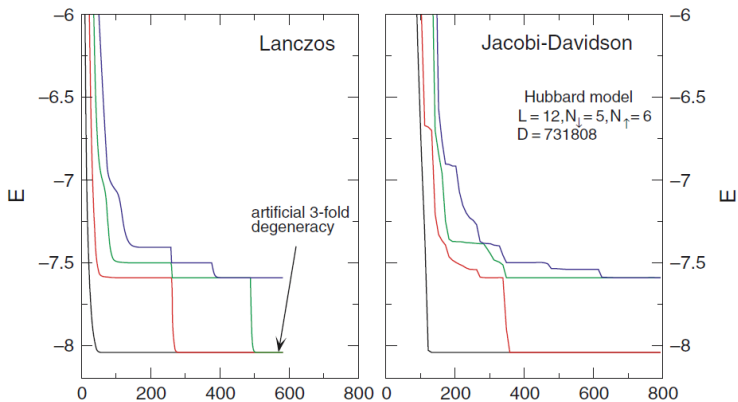
- 1 Introduction
- 2 Some Ingredients in ED
 - Basis Representation
 - Hamiltonian Matrix
 - Symmetries
 - Hamiltonian Matrix
 - Diagonalization Routines
- 3 Lanczos Algorithm
 - Basis of Lanczos
 - Loss of Orthogonality and Ghosts
- 4 Miscellaneous Applications
 - Green's Function
 - Finite Temperature Lanczos Methods
 - Time-Dependent Lanczos



Round-Off Errors and Ghosts

- In exact arithmetic, the basis set $\{\phi_i\}$ are orthogonal, and the Lanczos scheme should never produce degenerate states.
- The loss of orthogonality is caused by the accumulation of round-off errors in the course of constructing the basis set.
- Once the ground state has converged, the vectors in the recursion tend to lose their orthogonality.
- Then the resulting matrix contains extra spurious eigenvalues, called “ghosts”, which are not real eigenvalues of H .
- The ghosts converge towards *real* eigenvalues of H with the iteration process continuing, and increase some states multiplicities.
- Checkpointing is useful when performing large-scale simulations.





Outline

- 1 Introduction
- 2 Some Ingredients in ED
 - Basis Representation
 - Hamiltonian Matrix
 - Symmetries
 - Hamiltonian Matrix
 - Diagonalization Routines
- 3 Lanczos Algorithm
 - Basis of Lanczos
 - Loss of Orthogonality and Ghosts
- 4 Miscellaneous Applications
 - Green's Function
 - Finite Temperature Lanczos Methods
 - Time-Dependent Lanczos



Besides using Lanczos to obtain the ground state of a Hamiltonian and some low-lying spectrum, we can use the algorithm for various purposes.



Outline

- 1 Introduction
- 2 Some Ingredients in ED
 - Basis Representation
 - Hamiltonian Matrix
 - Symmetries
 - Hamiltonian Matrix
 - Diagonalization Routines
- 3 Lanczos Algorithm
 - Basis of Lanczos
 - Loss of Orthogonality and Ghosts
- 4 Miscellaneous Applications
 - **Green's Function**
 - Finite Temperature Lanczos Methods
 - Time-Dependent Lanczos



Green's Function - Continued Fraction

We want to calculate

$$G(\omega) = \langle \psi_0 | O^\dagger \frac{1}{\omega - H + E_0} O | \psi_0 \rangle$$

Define the normalized initial state as

$$|\phi_0\rangle := \frac{1}{\sqrt{\langle \psi_0 | O^\dagger O | \psi_0 \rangle}} O | \psi_0 \rangle$$

Then

$$G(\omega) = \langle \psi_0 | O^\dagger O | \psi_0 \rangle \langle \phi_0 | \frac{1}{z - H} | \phi_0 \rangle = \langle \psi_0 | O^\dagger O | \psi_0 \rangle (z - H)_{00}^{-1}$$

with $z = \omega + E_0$, and

$$z - H = \begin{pmatrix} z - a_0 & -b_1 & 0 & \dots \\ -b_1 & z - a_1 & -b_2 & \dots \\ 0 & -b_2 & z - a_2 & \dots \\ \vdots & \vdots & \vdots & \ddots \end{pmatrix}$$



$$z - H = \begin{pmatrix} z - a_0 & -b_1 & 0 & \dots \\ -b_1 & z - a_1 & -b_2 & \dots \\ 0 & -b_2 & z - a_2 & \dots \\ \vdots & \vdots & \vdots & \ddots \end{pmatrix}$$

$$\begin{aligned} (z - H)_{00}^{-1} &= \frac{\det D_1}{\det(z - H)} = \frac{\det D_1}{(z - a_0) \det D_1 - b_1^2 \det D_2} = \frac{1}{z - a_0 - b_1^2 \frac{\det D_2}{\det D_1}} \\ &= \frac{1}{z - a_0 - \frac{b_1^2}{z - a_1 - \frac{b_2^2}{z - a_2 - \dots}}} \end{aligned}$$

More details, see [Elbio Dagotto, RMP 66, 763 \(1994\)](#)



Outline

- 1 Introduction
- 2 Some Ingredients in ED
 - Basis Representation
 - Hamiltonian Matrix
 - Symmetries
 - Hamiltonian Matrix
 - Diagonalization Routines
- 3 Lanczos Algorithm
 - Basis of Lanczos
 - Loss of Orthogonality and Ghosts
- 4 Miscellaneous Applications
 - Green's Function
 - **Finite Temperature Lanczos Methods**
 - Time-Dependent Lanczos



Finite Temperature Lanczos Methods

$$\langle A \rangle = \frac{1}{Z} \sum_{n=1}^N \langle n | A e^{-\beta H} | n \rangle, \quad Z = \sum_{n=1}^N \langle n | e^{-\beta H} | n \rangle$$

- Finite T (FTLM)

$$\langle A \rangle = \frac{1}{Z} \sum_{r=1}^R \sum_{j=0}^M e^{-\beta \epsilon_j^r} \langle r | \psi_j^r \rangle \langle \psi_j^r | A | r \rangle,$$

$$Z = \sum_{r=1}^R \sum_{j=0}^M e^{-\beta \epsilon_j^r} \left| \langle r | \psi_j^r \rangle \right|^2,$$

where

- ▶ \sum_r is a stochastic sampling over starting vectors $|r\rangle$.
- ▶ $|\psi_j^r\rangle$ and ϵ_j^r are obtained in Lanczos algorithm with the initial state $|r\rangle$.
- ▶ M is the Lanczos cutoff.

- Low T (LTLM)

$$\langle A \rangle = \frac{1}{Z} \sum_{r=1}^R \sum_{i=0}^M \sum_{j=0}^M e^{-\beta \epsilon_i^r / 2} e^{-\beta \epsilon_j^r / 2} \langle r | \psi_i^r \rangle \langle \psi_j^r | A | \psi_i^r \rangle \langle \psi_i^r | r \rangle$$



Outline

- 1 Introduction
- 2 Some Ingredients in ED
 - Basis Representation
 - Hamiltonian Matrix
 - Symmetries
 - Hamiltonian Matrix
 - Diagonalization Routines
- 3 Lanczos Algorithm
 - Basis of Lanczos
 - Loss of Orthogonality and Ghosts
- 4 Miscellaneous Applications
 - Green's Function
 - Finite Temperature Lanczos Methods
 - Time-Dependent Lanczos



Time-Dependent Lanczos

A time-dependent Schrödinger equation,

$$i\frac{\partial\psi(t)}{\partial t} = H(t)\psi(t), \quad |\psi(t)\rangle = \mathcal{T} \left[e^{-i\int_{t_0}^t H(t')dt'} \right] |\psi(t=t_0)\rangle$$

The time evolution of $|\psi(t)\rangle$ can be approached by step-wise change of time t in small time increments δt .

$$|\psi(t + \delta t)\rangle \simeq e^{-iH(t)\delta t}|\psi(t)\rangle \simeq \sum_{l=1}^M |l\rangle\langle l|e^{-iH(t)\delta t}|\psi(t)\rangle = \sum_{l=1}^M e^{-i\epsilon_l\delta t}|l\rangle\langle l|\psi(t)\rangle,$$

where $|l\rangle, \epsilon_l, M$ are Lanczos *eigenvectors* and *eigenvalues* of the tridiagonal matrix with dimension M , obtained by Lanczos iterations. $|\psi(t)\rangle$ is served as the initial state.

The unitarity of the time-evolution operator is preserved in this method.



For

$$|\psi(t + \delta t)\rangle \simeq \sum_{l=1}^M e^{-i\epsilon_l \delta t} |l\rangle \langle l|\psi(t)\rangle,$$

suppose $\{|n\rangle\}$ are the bases in Krylov space. The relations between the Krylov basis and the original basis can be obtained in the Lanczos iteration successively:

$$|n\rangle = \sum_i a_i^{(n)} |i\rangle$$

$$|0\rangle = |\psi(t)\rangle, \quad |l\rangle = \sum_n A_{nl} |n\rangle \quad (\text{column style})$$

$$\langle l|\psi(t)\rangle = \langle l|0\rangle = A_{0l}^* = A_{0l} \quad (\text{real vectors})$$

So

$$|\psi(t + \delta t)\rangle \simeq \sum_n \sum_i \sum_{l=1}^M e^{-i\epsilon_l \delta t} A_{0l} A_{nl} a_i^{(n)} |i\rangle.$$



For more details, see

Peter Prelovšek and Janez Bonča, *Ground State and Finite Temperature Lanczos Methods*, arXiv:1111.5931.



T H A N K Y O U



Solving Out-Of-Equilibrium Quantum Problems via Time-Dependent Lanczos Method: II

Hantao Lu

Lanzhou University

CSRC Workshop on Quantum Non-Equilibrium Phenomena:
Methods and Applications, 17-21 June 2019



Outline

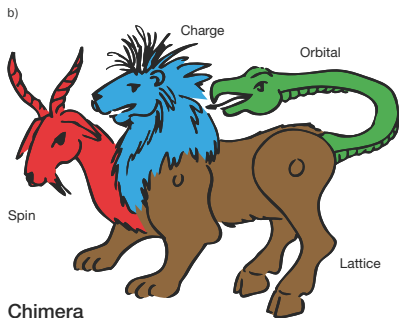
- 1 Introduction: Ultrafast Spectroscopy
- 2 The Probe Dependence of the Optical Conductivity in Nonequilibrium
 - Optical Conductivity
 - Pump-Probe Method
 - Results in Nonequilibrium
 - Two Different Theoretical Approaches
 - Conclusions



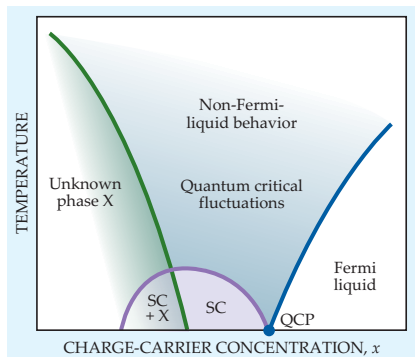
Why are we interested in (or do we need) ultrafast dynamics?



Complexity in Correlated Electronic Systems



Interplay between various degrees of freedom



A generic phase diagram



Using ultrafast spectroscopy, in principle, we can

- Decouple various degrees of freedom
- Selective examinations
- Study their cooperative or competitive interplays
- Nonequilibrium dynamics

Next, we will give some examples...



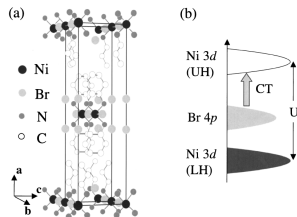
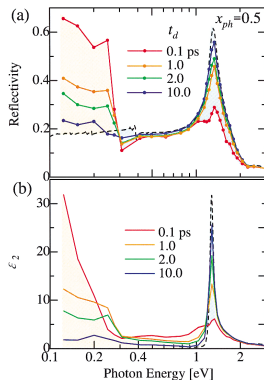
Transient Insulator-to-Metal transition I

VOLUME 91, NUMBER 5

PHYSICAL REVIEW LETTERS

week ending
1 AUGUST 2003

Ultrafast Optical Switching to a Metallic State by Photoinduced Mott Transition in a Halogen-Bridged Nickel-Chain Compound

S. Iwai,^{1,2} M. Ono,³ A. Maeda,³ H. Matsuzaki,³ H. Kishida,^{3,4} H. Okamoto,^{1,3,5} and Y. Tokura^{1,6}

Transient Insulator-to-Metal transition II

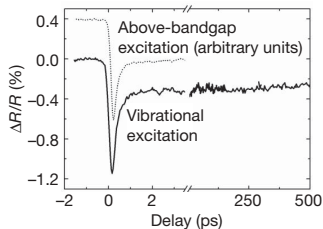
nature

Vol 449 | 6 September 2007 | doi:10.1038/nature06119

LETTERS

Control of the electronic phase of a manganite by mode-selective vibrational excitation

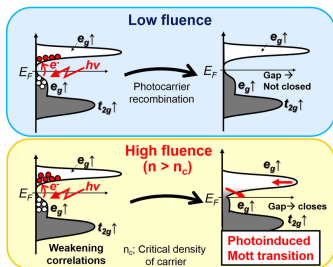
Matteo Rini¹, Ra'anan Tobey², Nicky Dean², Jiro Itatani^{1,3}, Yasuhide Tomioka⁴, Yoshinori Tokura^{4,5}, Robert W. Schoenlein¹ & Andrea Cavalleri^{2,6}



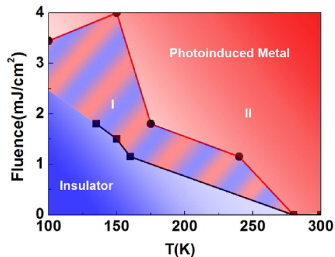
“Phonon-driven”
insulator-to-metal transition:
 $\text{Pr}_{0.7}\text{Ca}_{0.3}\text{MnO}_3$.

Solid line: 17.5 μm (pumping wavelength); dotted line: 800 nm.





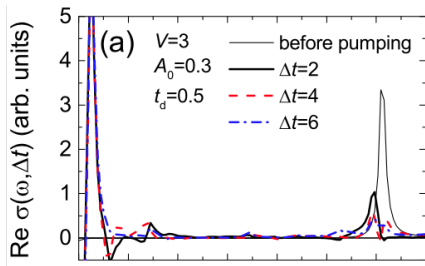
On BaFeO₃ thin films. Source: T. Tsuyama *et al.*, Phys. Rev. Lett. **116**, 256402 (2016)



On VO₂(B). Source: J. Lourembam *et al.*, Sci. Rep. **6**, 25538 (2016)

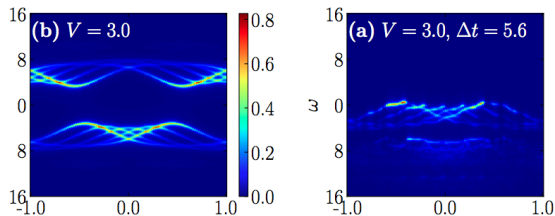


What does it Look like?



1D Extended Hubbard model.
 $U = 10$, $L = 14$; periodic BC.

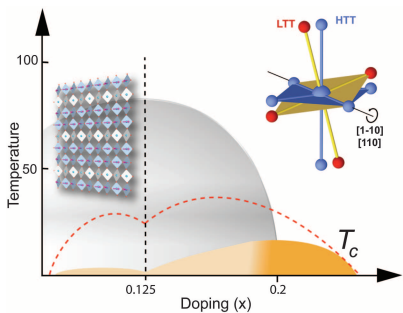
Source: LHT *et al*, Phys. Rev. B
91, 245117 (2015)



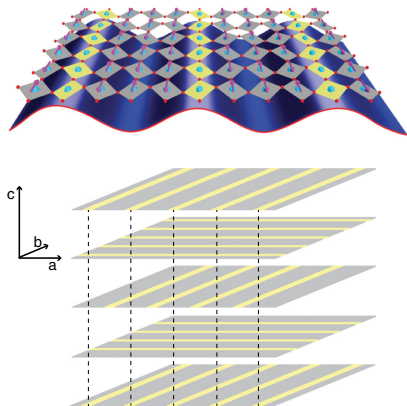
Single-particle spectrum. $L = 10$,
 twisted BC. (b) Ground state;
 $I_+(k, \omega) + I_-(k, \omega)$; (a) Pump
 applied, I_- only. Can Shao *et al.*,
 in preparation.



“Light-Induced Superconductivity” in $\text{LESCE}_{1/8}$



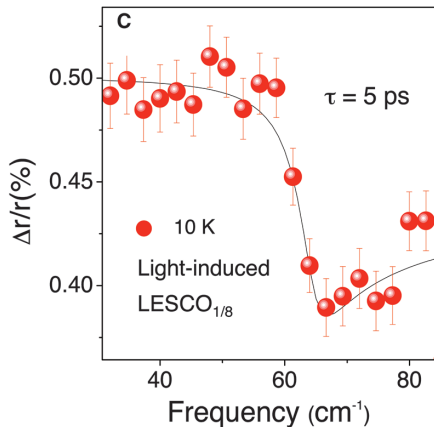
$\text{La}_{1.8-x}\text{Eu}_{0.2}\text{Sr}_x\text{CuO}_4$ (LESCO_x) phase diagram and low-temperature tetragonal (LTT) distortion



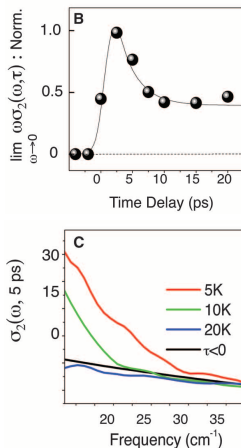
schematic drawing of stripe phase

It was believed that stripes are pinned by LTT.





transient *c*-axis reflectance: the signal of Josephson plasma resonance



imaginary part of optical conductivity $\sigma_2(\omega)$

D. Fausti *et al.*, Science **331**, 189 (2011)



Theoretical Challenges

In nonequilibrium strongly correlated systems, we have to deal with nonperturbative effects which can come from:

- Correlation effects
- Nonlinear effects due to strong external fields: redistribution of spectral weight ...
- In ultrafast spectroscopy, additionally we have to follow closely the rapid microscopical changes, not only their long-time-average behaviors.

Are we calculating the same entity as the one measured in experiments? (Ref. "Lectures on the non-equilibrium theory of condensed matter" by L. Bányai)



Theoretical Challenges

In nonequilibrium strongly correlated systems, we have to deal with nonperturbative effects which can come from:

- Correlation effects
- Nonlinear effects due to strong external fields: redistribution of spectral weight ...
- In ultrafast spectroscopy, additionally we have to follow closely the rapid microscopical changes, not only their long-time-average behaviors.

Are we calculating the same entity as the one measured in experiments? (Ref. "Lectures on the non-equilibrium theory of condensed matter" by L. Bányai)

Methods

- Exact diagonalization (ED)
- Time-dependent density-matrix renormalization group (tDMRG)
- Nonequilibrium dynamical mean-field theory (nDMFT)
- Time-dependent DFT
- Hydrodynamical approach
-



Outline

1 Introduction: Ultrafast Spectroscopy

2 The Probe Dependence of the Optical Conductivity in Nonequilibrium

- Optical Conductivity
- Pump-Probe Method
- Results in Nonequilibrium
- Two Different Theoretical Approaches
- Conclusions



Outline

1 Introduction: Ultrafast Spectroscopy

2 The Probe Dependence of the Optical Conductivity in Nonequilibrium

- **Optical Conductivity**
- Pump-Probe Method
- Results in Nonequilibrium
- Two Different Theoretical Approaches
- Conclusions



- An operational definition

$$\mathbf{j} = \sigma \mathbf{E}$$

Note that the time-reversal symmetry is explicitly broken!



- An operational definition

$\sigma(\omega)$ measures the response of the system with respect to a monochromatic perturbation field $E(t) \sim e^{-i\omega t}$:

$$\mathbf{j}(\omega) = \sigma(\omega) \mathbf{E}(\omega)$$



- An operational definition

$\sigma(\omega)$ measures the response of the system with respect to a monochromatic perturbation field $E(t) \sim e^{-i\omega t}$:

$$\mathbf{j}(\omega) = \sigma(\omega) \mathbf{E}(\omega)$$

- Linear response theory (fluctuation-dissipation theorem)

Kubo (1957) told us that the conductivity can be calculated microscopically in terms of the current-current correlations (KF) ($\mathcal{H} \sim \mathbf{j} \cdot \mathbf{A}$):

$$\begin{aligned} \sigma(\omega) &\sim \frac{1}{\omega L} \int_0^{+\infty} e^{i\omega t} \langle [j(t), j(0)] \rangle dt \\ &= \frac{i}{\omega L} \int_{-\infty}^{+\infty} e^{i\omega t} (-i)\theta(t) \langle [j(t), j(0)] \rangle dt \\ &= \frac{i}{\omega L} \chi(\omega) \end{aligned}$$



However, in nonequilibrium due to the absence of the time translation invariance, a *two-time response function* is required:

$$\mathbf{j}(t') = \int_{-\infty}^{t'} \sigma(t', t) \mathbf{E}(t) dt.$$

The response function $\sigma(t', t)$ measures the current response at t' with respect to a perturbation of an *unit pulse* at t .



However, in nonequilibrium due to the absence of the time translation invariance, a *two-time response function* is required:

$$\mathbf{j}(t') = \int_{-\infty}^{t'} \sigma(t', t) \mathbf{E}(t) dt.$$

The response function $\sigma(t', t)$ measures the current response at t' with respect to a perturbation of an *unit pulse* at t .

Consequently, no unique definition for the time-dependent optical conductivity in the *frequency space*.

e.g., see [M. Eckstein et al., PRB 81, 115131 \(2010\)](#); [Z. Lenarčič et al., PRB 89, 125123 \(2014\)](#)

We choose the one which reflects the causality ([Z. Lenarčič et al., 2014](#))

$$\sigma(\omega, t) := \int_0^{\infty} \sigma(t + s, t) e^{i\omega s} ds$$



From

$$j(t') = \int_{-\infty}^{t'} \sigma(t', t) E(t) dt, \quad \sigma(\omega, t) = \int_0^{\infty} \sigma(t+s, t) e^{i\omega s} ds$$

The Fourier transformation produces (t_0 can be $-\infty$, t_M can be $+\infty$)

$$j(\omega) = \int_{t_0}^{t_M} \sigma(\omega, t'') E(t'') e^{i\omega t''} dt'',$$



From

$$j(t') = \int_{-\infty}^{t'} \sigma(t', t) E(t) dt, \quad \sigma(\omega, t) = \int_0^{\infty} \sigma(t+s, t) e^{i\omega s} ds$$

The Fourier transformation produces (t_0 can be $-\infty$, t_M can be $+\infty$)

$$j(\omega) = \int_{t_0}^{t_M} \sigma(\omega, t'') E(t'') e^{i\omega t''} dt'',$$

- With time translational invariant: $\sigma(\omega, t) = \sigma(\omega)$, we return back

$$j(\omega) = \sigma(\omega) E(\omega).$$



From

$$j(t') = \int_{-\infty}^{t'} \sigma(t', t) E(t) dt, \quad \sigma(\omega, t) = \int_0^{\infty} \sigma(t+s, t) e^{i\omega s} ds$$

The Fourier transformation produces (t_0 can be $-\infty$, t_M can be $+\infty$)

$$j(\omega) = \int_{t_0}^{t_M} \sigma(\omega, t'') E(t'') e^{i\omega t''} dt'',$$

- With time translational invariant: $\sigma(\omega, t) = \sigma(\omega)$, we return back

$$j(\omega) = \sigma(\omega) E(\omega).$$

- What about the general case?



Recall that

$$j(\omega) = \int_{t_0}^{t_M} \sigma(\omega, t'') E(t'') e^{i\omega t''} dt''$$

In order to locate $\sigma(\omega, t)$, an obvious choice is to use the δ -electronic field:
 $E(t'') \sim \delta(t'' - t)$:

$$j(\omega) = \sigma(\omega, t) e^{i\omega t} = \sigma(\omega, t) E(\omega) = \sigma(\omega, t) (i\omega A(\omega))$$

\Downarrow

$$\boxed{\sigma(\omega, t) = j(\omega) / i\omega A(\omega)}$$



Outline

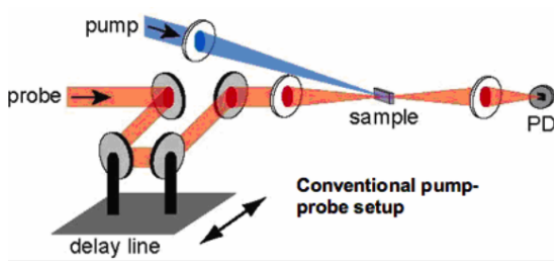
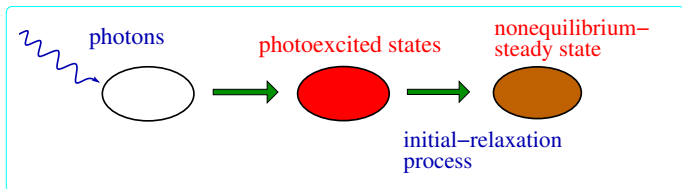
1 Introduction: Ultrafast Spectroscopy

2 The Probe Dependence of the Optical Conductivity in Nonequilibrium

- Optical Conductivity
- **Pump-Probe Method**
- Results in Nonequilibrium
- Two Different Theoretical Approaches
- Conclusions



Pump-Probe Setup



Strategy: Weak Pulse as a Probe

Applying a weak probing pulse $A_{\text{probe}}(t)$ (in terms of the vector potential):

$$\begin{array}{ccc}
 j_{\text{probe}}(t) & \xrightarrow{\text{Fourier transformation}} & j_{\text{probe}}(\omega), \\
 A_{\text{probe}}(t) & \xrightarrow{\text{Fourier transformation}} & A_{\text{probe}}(\omega), \\
 & \downarrow & \\
 \sigma(\omega) \sim j_{\text{probe}}(\omega)/i(\omega + i\eta)LA_{\text{probe}}(\omega) & & \\
 E(\omega) \sim i\omega A(\omega) & &
 \end{array}$$

The current operator reads

$$\hat{j}(t) \sim \frac{\delta H(t)}{\delta A(t)} = -it_h \sum \left[e^{iA(t)} c_{i,\sigma}^\dagger c_{i+1,\sigma} - \text{H.c.} \right].$$



Strategy: Weak Pulse as a Probe

Applying a weak probing pulse $A_{\text{probe}}(t)$ (in terms of the vector potential):

$$\begin{array}{ccc}
 j_{\text{probe}}(t) & \xrightarrow{\text{Fourier transformation}} & j_{\text{probe}}(\omega), \\
 A_{\text{probe}}(t) & \xrightarrow{\text{Fourier transformation}} & A_{\text{probe}}(\omega), \\
 & \downarrow & \\
 \sigma(\omega) \sim j_{\text{probe}}(\omega)/i(\omega + i\eta)LA_{\text{probe}}(\omega) & & \\
 E(\omega) \sim i\omega A(\omega) & &
 \end{array}$$

The current operator reads

$$\hat{j}(t) \sim \frac{\delta H(t)}{\delta A(t)} = -it_h \sum \left[e^{iA(t)} c_{i,\sigma}^\dagger c_{i+1,\sigma} - \text{H.c.} \right].$$

We call it the pump-probe (PP) method.

Note that in the Fourier transformation, the damping factor $e^{-\eta t}$ is also added to $j_{\text{probe}}(t)$ and $A_{\text{probe}}(t)$, where $\eta \sim 1/L$.



Time-dependent Lanczos method

T. J. Park and J. C. Light, *The Journal of Chemical Physics* **85**, 5870 (1986)

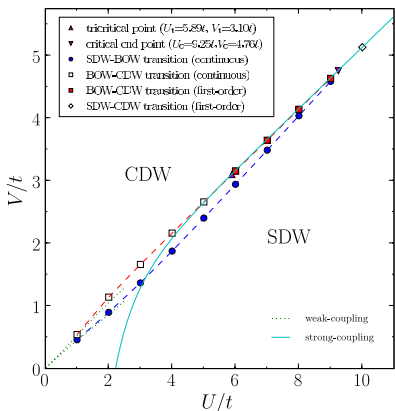
$$i\frac{\partial\psi(t)}{\partial t} = H(t)\psi(t).$$

We approximate the time evolution of $|\psi(t)\rangle$ by step-wise change of time t in small increment δt . At each step, Lanczos basis with dimension M are generated to follow the evolution

$$|\psi(t + \delta t)\rangle \simeq e^{-iH(t)\delta t}|\psi(t)\rangle \simeq \sum_{l=1}^M e^{-i\epsilon_l\delta t}|\phi_l\rangle\langle\phi_l|\psi(t)\rangle.$$



One-Dimensional Half-Filled Extended Hubbard Model



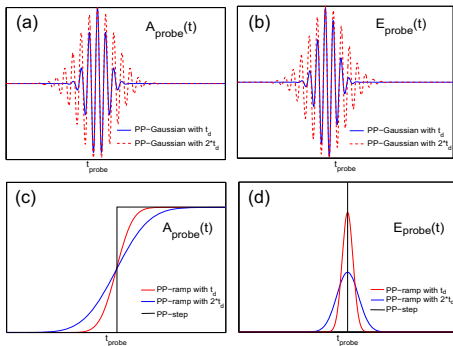
- Hopping: $-t_h \sum_i c_{i,\sigma}^\dagger c_{i+1,\sigma} + \text{H.c.}$
- U -term: $U \sum_i n_{i\uparrow} n_{i\downarrow}$
- V -term: $V \sum_i (n_i - 1)(n_{i+1} - 1)$

First order phase transition in equilibrium happens around $U \approx 2V$ between SDW and CDW, driven by the competition between **energy cost** for doublon generation and **energy reward** due to the attraction between doublon-holon pairs.

S. Ejima and S. Nishimoto, PRL **99**, 216403 (2007)



Two types of the probe pulse



- Gaussian pulse (PP-Gaussian)

$$A_{\text{probe}}(t) = A_0 e^{-(t-t_0)^2/2t_d^2} \cos[\omega(t-t_0)],$$

$$t_d \rightarrow 0, \quad A_{\text{probe}}(t) \rightarrow \delta(t-t_0)$$

- Step-like pulse (PP-ramp & -step)

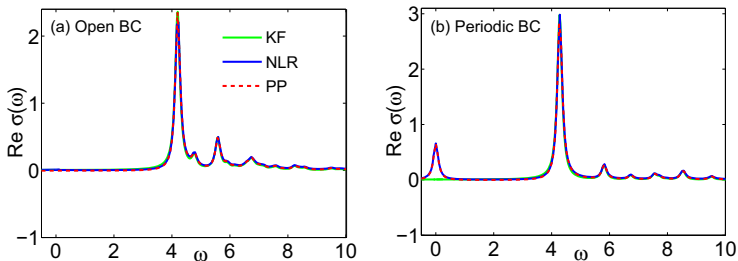
$$A_{\text{probe}} \sim A_{0,\text{step}} \theta(t-t_0),$$

$$E_{\text{probe}}(t) \sim \delta(t-t_0)$$

Schematic illustration of $A_{\text{probe}}(t)$ and $E_{\text{probe}}(t)$ for the Gaussian pulse ((a), (b)) and step-like pulse ((c), (d)) with various widths.



Illustration in the Equilibrium ($T = 0$)



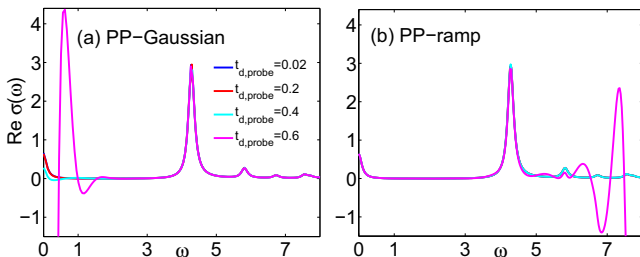
(a) open BC; (b) periodic BC. $L = 10$, $U = 10$, $V = 4.5$; half-filling. Note that there is nonzero Drude weight in the periodic BC for finite systems even at the insulating phase. In equilibrium both NLR and VNLR produce identical results, which also coincide with the PP method.

- (N)KF: (nonequilibrium) Kubo formula
- NLR: nonequilibrium linear response
- VNLR: a variant of NLR

Details will be explained later.



Probing-Pulse-Width Dependence



$L = 10$, $U = 10$, $V = 4.5$, half-filling & $T = 0$. (a) By PP-Gaussian with $\omega_{\text{probe}} = 10$, and $A_{0,\text{probe}} = 1.0 \times 10^{-6}$. (b) By PP-ramp with $A_{0,\text{step}} = 1.0 \times 10^{-4}$.

Finite width affects $A_{\text{probe}}(\omega)$:

- PP-Gaussian: a variance of $1/t_{d,\text{probe}}^2$ around ω_{probe}
- PP-ramp: $A_{\text{probe}}(\omega)$ exponentially decays with rate $\sim t_{d,\text{probe}}^2$

Basically, with $t_{d,\text{probe}} \rightarrow 0$, they are converged *in equilibrium*.



Generalize to Nonequilibrium: the PP Method

Towards nonequilibrium:

$$\sigma(\omega, t_{\text{probe}}) = \frac{j_{\text{probe}}(\omega, t_{\text{probe}})}{i(\omega + i\eta)LA_{\text{probe}}(\omega)},$$

where t_{probe} is the probing time.

$$j_{\text{probe}}(t') = \int_{t_0}^{t'} \sigma(t', t'') E_{\text{probe}}(t'') dt'',$$

$$j_{\text{probe}}(\omega) = \int_{t_0}^{t_M} j_{\text{probe}}(t') e^{i\omega t'} dt' = \int_{t_0}^{t_M} \sigma(\omega, t'') E_{\text{probe}}(t'') e^{i\omega t''} dt''$$

In order to obtain $\sigma(\omega, t)$, a narrow probe pulse at the moment t is preferred, which is consistent with the ultrafast spectroscopy setup.

Checking...

see [Can Shao et al., PRB 93, 195144 \(2016\)](#)



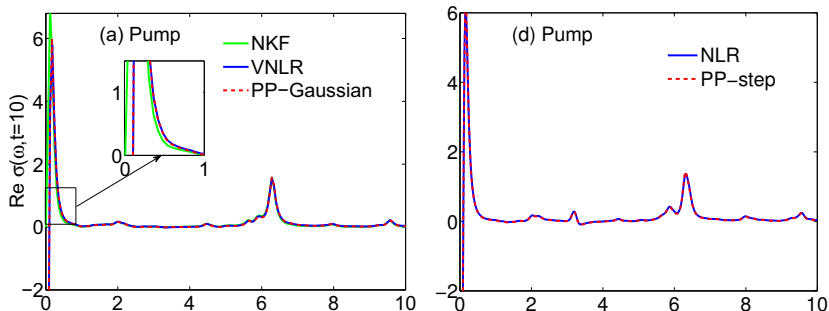
Outline

1 Introduction: Ultrafast Spectroscopy

2 The Probe Dependence of the Optical Conductivity in Nonequilibrium

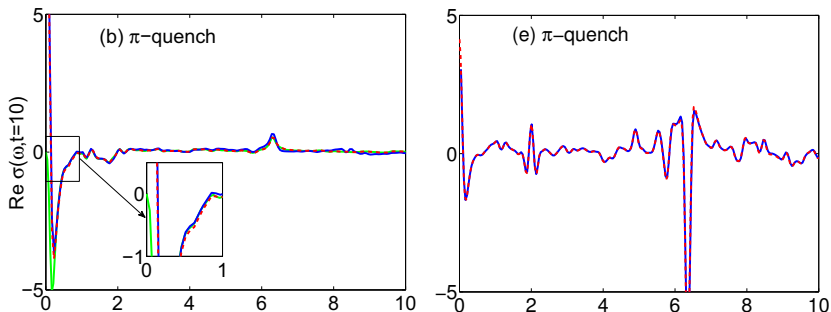
- Optical Conductivity
- Pump-Probe Method
- **Results in Nonequilibrium**
- Two Different Theoretical Approaches
- Conclusions





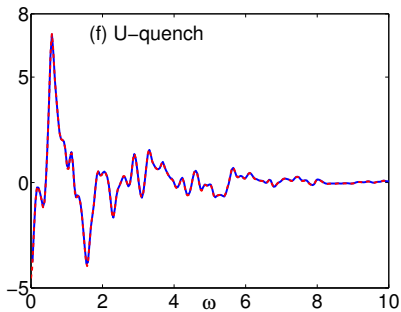
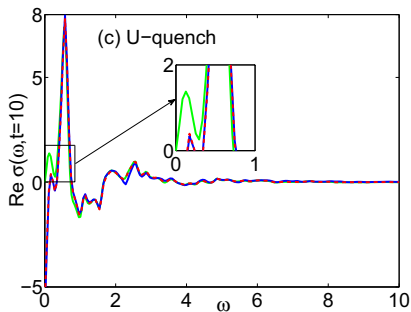
A pump case: $A_{0,pump} = 0.2$, $\omega_{pump} = 6.29$ (resonant frequency), and $t_{d,pump} = 0.5$. In PP-Gaussian, $t_{d,probe} = 0.02$. Parameters: $L = 10$, $U = 10$, $V = 3$. Half-filling.





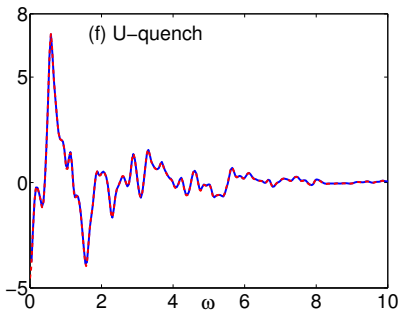
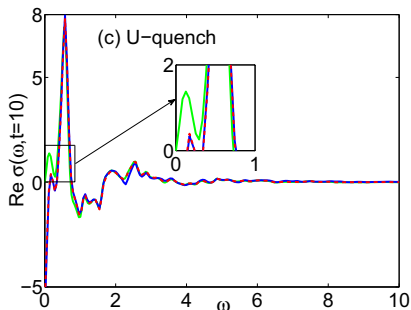
A π -quench in the hopping terms is applied at $t = 0$. Parameters: $L = 10$, $U = 10$, $V = 3$. Half-filling.





A U -quench: U changes from 10 to 4 at $t = 0$. Parameters: $L = 10$, $V = 3$. Half-filling.





A U -quench: U changes from 10 to 4 at $t = 0$. Parameters: $L = 10$, $V = 3$. Half-filling.

Different probing pulses (Gaussian vs step-like) produce different $\sigma(\omega, t)$!

We have verified numerically

$$\text{NLR} \sim \text{PP-step}$$

$$\text{VNLR} \sim \text{PP-Gaussian as } t_{d,\text{probe}} \rightarrow 0$$



Outline

1 Introduction: Ultrafast Spectroscopy

2 The Probe Dependence of the Optical Conductivity in Nonequilibrium

- Optical Conductivity
- Pump-Probe Method
- Results in Nonequilibrium
- **Two Different Theoretical Approaches**
- Conclusions



Two Different Theoretical Approaches

$$j(t') = \int_{-\infty}^{t'} \sigma(t', t) E(t) dt$$

$$\sigma(\omega, t) = \int_0^{\infty} \sigma(t+s, t) e^{i\omega s} ds$$

- the nonequilibrium linear response (NLR) (for a pure state)

$$\sigma(t', t) = \frac{1}{L} \left[\langle \psi(t') | \tau | \psi(t') \rangle + \int_t^{t'} \chi(t', t'') dt'' \right], \quad t' \geq t$$

where in the diamagnetic term, $\tau = t_h \sum_{i,\sigma} (c_{i+1,\sigma}^\dagger c_{i,\sigma} + \text{H.c.}) \propto$ kinetic energy,
and

$$\begin{aligned} \chi(t', t'') &= -i\theta(t' - t'') \langle \psi(t) | [j^I(t'), j^I(t'')] | \psi(t) \rangle, \\ j^I(t') &= U(t, t') j U(t', t). \end{aligned}$$

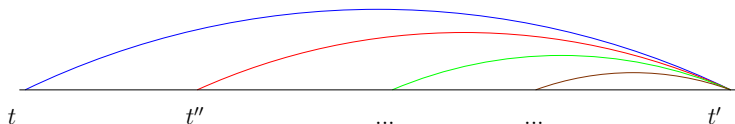
e.g., see [Z. Lenarčič et al., PRB 89, 125123 \(2014\)](#)



The Temporal Correlations in NLR

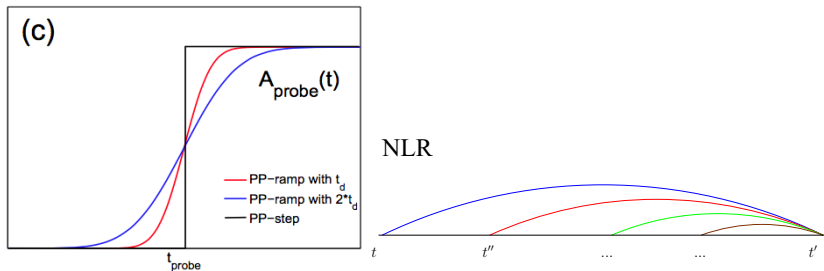
$$\sigma(t', t) = \frac{1}{L} \left[\langle \psi(t') | \tau | \psi(t') \rangle + \int_t^{t'} \chi(t', t'') dt'' \right]$$

NLR



The Temporal Correlations in NLR

$$\sigma(t', t) = \frac{1}{L} \left[\langle \psi(t') | \tau | \psi(t') \rangle + \int_t^{t'} \chi(t', t'') dt'' \right]$$



We have learned that PP-step \sim NLR; the two are consistent.



NKF and VNLR

- A generalized Kubo formula (NKF)

$$\text{Re } \sigma_{\text{reg}}(\omega, t) = \frac{1}{\omega L} \text{Im} \int_0^{\infty} i e^{i(\omega+i\eta)s} \langle \psi(t) | [j'(t+s), j'(t)] | \psi(t) \rangle ds$$

e.g., in [D. De Filippis et al., PRL 109, 176402 \(2012\)](#)

The generalized Kubo formula actually can be derived from a variant of the response function (VNLR):

$$\tilde{\sigma}(t', t) = \frac{1}{L} \left[\langle \psi(t') | \tau | \psi(t') \rangle + \int_t^{t'} \chi(t'', t) dt'' \right], \quad t' \geq t$$

where

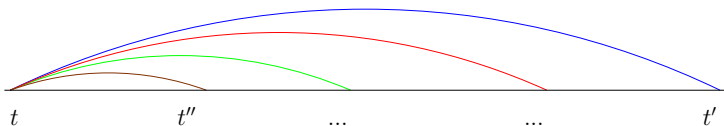
$$\chi(t'', t) = -i\theta(t'' - t) \langle \psi(t) | [j'(t''), j'(t)] | \psi(t) \rangle$$



The Temporal Correlations in VNLR

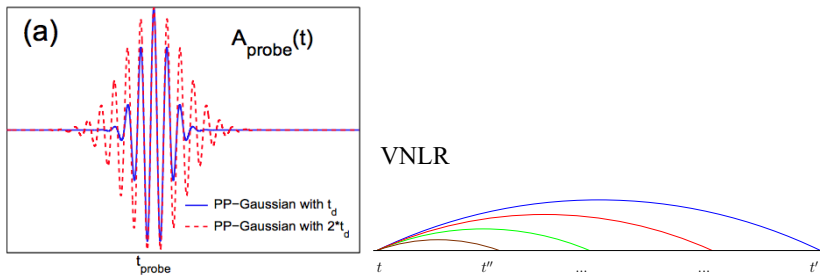
$$\tilde{\sigma}(t', t) = \frac{1}{L} \left[\langle \psi(t') | \tau | \psi(t') \rangle + \int_t^{t'} \chi(t'', t) dt'' \right]$$

VNLR



The Temporal Correlations in VNLR

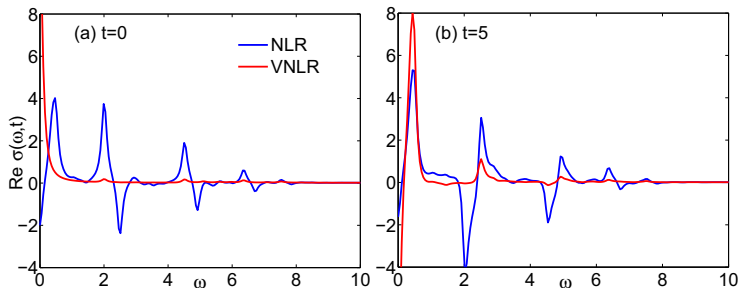
$$\tilde{\sigma}(t', t) = \frac{1}{L} \left[\langle \psi(t') | \tau | \psi(t') \rangle + \int_t^{t'} \chi(t'', t) dt'' \right]$$



We can show that the δ -like **vector potential** A (PP-Gaussian when $t_d \rightarrow 0$) \sim VNLR.



Additional Note



U -quench from $U = 0$ to 2 at $t = 0$. Parameters: $L = 10$, $V = 0$.

Message: In nonequilibrium, the difference between NLR (PP-step) and VNLR (PP-Gaussian) can be significant in the early stage of the evolution.



Outline

1 Introduction: Ultrafast Spectroscopy

2 The Probe Dependence of the Optical Conductivity in Nonequilibrium

- Optical Conductivity
- Pump-Probe Method
- Results in Nonequilibrium
- Two Different Theoretical Approaches
- **Conclusions**



Conclusions

- We have raised the issue of the probe-pulse dependence in the calculation of the time-resolved optical conductivity $\sigma(\omega, t)$.
- Different formulas for $\sigma(\omega, t)$ in the literature actually describe the outcomes of different probing pulses.
- The nature of the probe pulses should be closely examined in the analysis of ultrafast THz spectroscopy data.



T H A N K Y O U

